THE JOURNAL OF BIOLOGICAL CHEMISTRY VOL. 292, NO. 9, pp. 3877–3887, March 3, 2017

P3h3-null and Sc65-null Mice Phenocopy the Collagen Lysine Under-hydroxylation and Cross-linking Abnormality of Ehlers-Danlos Syndrome Type VIA*

Received for publication, October 6, 2016, and in revised form, January 18, 2017 Published, JBC Papers in Press, January 23, 2017, DOI 10.1074/jbc.M116.762245

David M. Hudson[‡1], **MaryAnn Weis**[‡], **Jyoti Rai**[‡], **Kyu Sang Joeng**[§], **Milena Dimori**[¶], **Brendan H. Lee**[§], **Roy Morello**[¶], **and David R. Eyre**[‡]

From the [‡]*Department of Orthopaedics and Sports Medicine, University of Washington, Seattle, Washington 98195, the* [§]*Department of Molecular and Human Genetics, Baylor College of Medicine, Houston, Texas 77030, and the* [¶]*Department of Physiology & Biophysics, University of Arkansas for Medical Sciences, Little Rock, Arkansas 72205*

Edited by Xiao-Fan Wang

Tandem mass spectrometry was applied to tissues from targeted mutant mouse models to explore the collagen substrate specificities of individual members of the prolyl 3-hydroxylase (P3H) gene family. Previous studies revealed that P3h1 preferentially 3-hydroxylates proline at a single site in collagen type I chains, whereas P3h2 is responsible for 3-hydroxylating multiple proline sites in collagen types I, II, IV, and V. In screening for collagen substrate sites for the remaining members of the vertebrate P3H family, P3h3 and Sc65 knock-out mice revealed a common lysine under-hydroxylation effect at helical domain cross-linking sites in skin, bone, tendon, aorta, and cornea. No effect on prolyl 3-hydroxylation was evident on screening the spectrum of known 3-hydroxyproline sites from all major tissue collagen types. However, collagen type I extracted from both *Sc65*$^{-/-}$ and *P3h3*$^{-/-}$ skin revealed the same abnormal chain pattern on SDS-PAGE with an overabundance of a γ_{112} cross-linked trimer. The latter proved to be from native molecules that had intramolecular aldol cross-links at each end. The lysine under-hydroxylation was shown to alter the divalent aldimine cross-link chemistry of mutant skin collagen. Furthermore, the ratio of mature HP/LP cross-links in bone of both *P3h3*$^{-/-}$ and *Sc65*$^{-/-}$ mice was reversed compared with wild type, consistent with the level of lysine under-hydroxylation seen in individual chains at cross-linking sites. The effect on cross-linking lysines was quantitatively very similar to that previously observed in EDS VIA human and *Plod1*$^{-/-}$ mouse tissues, suggesting that P3H3 and/or SC65 mutations may cause as yet undefined EDS variants.

The collagen family of proteins has evolved into many different genes and gene translational products each with variably regulated post-translational modifications (1, 2). Even within a single genetic type of collagen, the post-translational quality of the protein is known to be regulated with a high degree of tissue specificity (3, 4). The functional significance of this post-translational variability is still not fully understood, although for fibril-forming collagens the number, placement, and chemistry of covalent intermolecular cross-links seem to be critically important regulators of tissue material properties and function (5–7).

In the last decade, new insights on the significance of a relatively rare collagen modification, prolyl 3-hydroxylation, came from the discovery that recessive forms of osteogenesis imperfecta (OI)[2] are caused by biallelic mutations in prolyl 3-hydroxylase 1 (P3H1; *Lepre1*), CRTAP (*Leprel3*), or CypB (*PPIB*) (8). These proteins, which form a P3H1 enzyme complex, act on nascent collagen chains in the ER (9). Mutations in at least 6 further genes that encode either enzymes (*e.g. PLOD2* encoding lysyl hydroxylase-2 (LH2) (10)) or chaperones (*e.g. FKBP10* encoding FKBP65 (11, 12)), needed for collagen modification, folding, transport, and normal mineralization, have been shown to cause OI variants. We have gained insights on the disease-causing mechanisms by analyzing tissue collagens from OI patients and mouse models of OI. For example, P3H1, CRTAP, and PPIB mutations all cause telopeptide lysine over-hydroxylation (5), whereas PLOD2 or FKBP10 mutations cause telopeptide lysine under-hydroxylation (10–12). A common effect from all these mutations is an altered collagen cross-linking chemistry. These findings suggest an interplay in the ER between the prolyl 3-hydroxylation complex and the lysyl hydroxylation machinery.

Human mutations in P3H2 (*Leprel1*) have been shown to cause the eye disorder high myopia (13–15). Two different P3H2 knock-out mice have so far been generated by separate laboratories, the first was embryonic lethal (16), whereas the second had no obvious phenotype (17). Mass spectral analysis of multiple tissues from the latter P3H2 knock-out mouse revealed that collagen types I, II, V, and IV lack 3-hydroxypro-

* This work was supported by grants from the National Institute of Arthritis and Musculoskeletal and Skin Diseases and Eunice Kennedy Shriver NICHD, National Institutes of Health NIAMS Grants AR037318 (to D. E.), AR036794 (to D. E.), AR060823 (to R. M.), and NICHD Grant HD070394 (to B. L. and D. E.). The authors declare that they have no conflicts of interest with the contents of this article. The content is solely the responsibility of the authors and does not necessarily represent the official views of the National Institutes of Health.

[1] To whom correspondence should be addressed. Tel.: 206-543-4700; Fax: 206-685-4700; E-mail: dmhudson@uw.edu.

[2] The abbreviations used are: OI, osteogenesis imperfecta; ER, endoplasmic reticulum; Sc65, synaptonemal complex 65; P3H1, P3H2, P3H3, prolyl 3-hydroxylases; LH1, LH2, lysyl hydroxylases; EDS, Ehlers-Danlos syndrome; 3Hyp, 3-hydroxyproline; Hyl, hydroxylysine; LP, lysyl pyridinoline; HP, hydroxylysyl pyridinoline.

line at all sites other than the few sites acted on by P3H1 (17). But so far, neither substrate specificity nor disease-associated mutations have been identified for P3H3. Recombinant P3H3 protein expressed in bacteria was reported to form insoluble aggregates with no detectable hydroxylating activity (18). The fifth remaining member of the gene family, synaptonemal complex 65 (Sc65), is a close homologue of Crtap with an apparent function in bone homeostasis (19), as well as a suspected role as an autoimmune target in membranous nephropathy (20). We recently reported suppressed collagen lysine hydroxylation in the Sc65-null mouse and evidence for complex formation between Sc65, P3H3, and potentially lysyl hydroxylase-1 (LH1) and CypB (21).

To understand more about the collagen substrate specificity of P3H3 and the function of Sc65, we screened tissues from Sc65- and P3h3-null mice using tandem mass spectrometry for collagen post-translational effects. The aim was to see if any known sites of 3-hydroxyproline in the various collagen types were under-hydroxylated and also if other post-translational modifications, in particular lysine modification and collagen cross-linking chemistry were affected. The results showed that both P3h3- and Sc65-null mice displayed a similar pattern of severe under-hydroxylation of lysines, particularly at cross-linking sites in type I collagen from bone, skin, dentin, cornea, and aorta. No loss of prolyl 3-hydroxylation was evident at any site accessible to tryptic peptide mass spectral screening of collagen types I, II, IV, and V from several tissue sources. The findings point to a complex evolution and interplay between the proteins forming the machinery of collagen prolyl 3-hydroxylation and lysyl hydroxylation in the ER.

Results

Generation of Sc65 and P3H3 Knock-out Mice—The murine *Leprel4* (Sc65) gene was inactivated by homologous recombination in ES cells using two approaches. The first mouse model was established via gene trap insertional mutagenesis (19), whereas the second was generated by introducing flanking *loxP* sites in the *Leprel4* gene (floxed) and then bred with a mouse ubiquitously expressing Cre-recombinase (21). Generation and initial characterization of each of these Sc65-null mouse models has been described (19, 21). The murine *Leprel2* (P3h3) gene was inactivated by homologous recombination in ES cells using BAC technology (Fig. 1*A*). Cross-breeding of heterozygous mice ($P3h3^{+/-}$) produced the null genotypes. Immunoblot analysis using a polyclonal P3H3 antibody against fractionated renal protein extracts showed absence of protein expression in the $P3h3^{-/-}$ mice (Fig. 1*B*). A 4 M guanidine HCl extract of fetal human cartilage was used as the positive control.

Both homozygous mouse strains, $Sc65^{-/-}$ and $P3h3^{-/-}$, were viable and showed no skeletal growth defects grossly or histologically or any other abnormalities when observed in the cage environment. $P3h3^{-/-}$ skin sections on H&E staining (Fig. 1*C*) showed some evidence of collagen fabric fragility (Fig. 1*C*), similar to that observed in $Sc65^{-/-}$ skin sections (21). Furthermore, on dissection, the skin of both homozygous null strains appeared to lack the structural integrity of normal mouse skin. Skin from $Sc65^{-/-}$ mice also proved on mechanical testing to fail at lower loads (21). Unless otherwise stated, the WT mouse

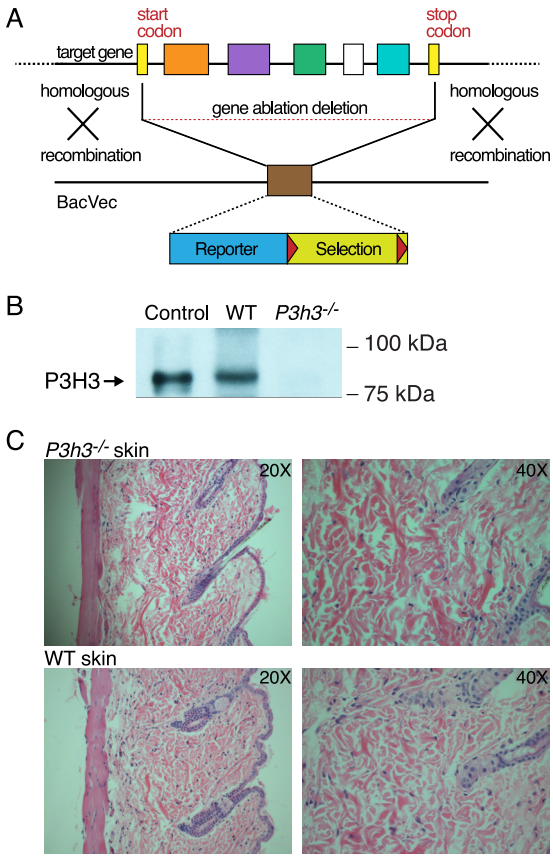

FIGURE 1. **Generation of $P3h3^{-/-}$ mice.** *A*, the *Leprel2* gene was inactivated by homologous recombination in ES cells using BAC technology. Mice were maintained on a C57/BL6J background. *B*, immunoblot analysis using a polyclonal P3H3 antibody against total protein extracts from whole kidneys of WT and $P3h3^{-/-}$ mice supported the loss of protein in the knock-out mice. Human fetal cartilage extract was loaded as a positive control marker for P3H3. *C*, representative H&E images of skin sections from $P3h3^{-/-}$ and WT mice.

genotype used in this study was $Sc65^{+/+}$. Tissue collagens from the heterozygote $P3h3^{+/-}$ mouse, which were determined to be indistinguishable from $Sc65^{+/+}$ mouse (WT) by collagen SDS-PAGE and mass spectral analysis, were also used as a control in this study where indicated.

Collagen Chain Profile on SDS-PAGE—Acid-extracted collagens from skin, bone, and tendon were resolved on SDS-PAGE to assess potential tissue-specific differences in the collagen cross-linking profiles. Reproducible and similar differences in collagen chain patterns were evident from skin of both $Sc65^{-/-}$ and $P3h3^{-/-}$ mice compared with their respective WT littermates (the latter patterns being indistinguishable). Significantly, a band we previously identified as the chain trimer, γ_{112} (12, 22), was reproducibly more prominent in the null mouse collagen extracts relative to the α and β bands (Fig. 2). The β_{12} component from both null strains was also noticeably depleted compared with WT in proportion with the increase in γ_{112}. From normal skin and tendon, the β-dimers are known to be the result of intramolecular aldol cross-link formation between allysines in α1-α1 and α1-α2 N-telopeptides. The shift from β_{12} to γ_{112} observed with the null mice suggested an effect on intermolecular cross-linking. We reported a similar banding pattern from fibromodulin null mouse tendons and concluded

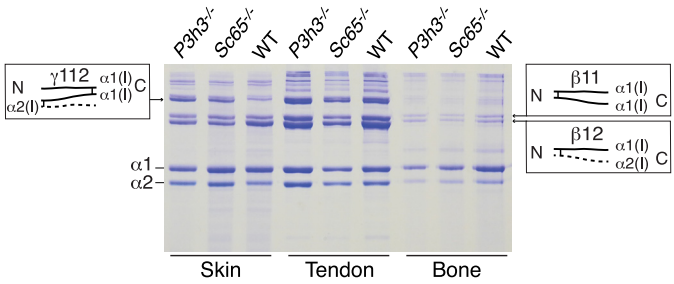

FIGURE 2. **SDS-PAGE reveals altered cross-linking in skin type I collagen from *P3h3*$^{-/-}$ and *Sc65*$^{-/-}$ mice.** As visualized by 6% SDS-PAGE, type I collagen from *P3h3*$^{-/-}$ and *Sc65*$^{-/-}$ mouse skin acid extracts reproducibly yielded more γ_{112} relative to WT. Accompanying this increased band intensity in knock-out mice skin is the decrease in β_{12} relative to WT mice. This shift in banding pattern is not observed in acid extracts of bone and tendon.

TABLE 1

Comparison of 3Hyp occupancy in collagens from *Sc65*$^{-/-}$, *P3h3*$^{-/-}$, and control mouse tissues

Percentage of 3Hyp at each major substrate site in type I collagen in tendon (T), bone (B), skin (Sk), kidney (K), cornea (Co), and sclera (Sc); type II collagen in cartilage (Cart), type IV collagen in kidney (K), and type V collagen in bone (B). Each percentage was determined based on the ratio of the *m/z* peaks of each post-translational variant from a minimum of three mice unless indicated. ([a]two mice; [b]one mouse).

Type I	α1(I)986				
	T	B	Sk	Co	Sc
Sc65$^{-/-}$	92.0±0.0%	91.3±5.5%	89.7±2.1%	95.0±2.0%	95.3±0.6%
Sc65$^{+/+}$	92.0±1.2%	91.3±5.5%	88.0±2.0%	95.0±0%	96.0±1.0%
P3h3$^{-/-}$	92±1.6%	97.3±1.2%	81.3±1.2%	n/a	n/a
P3h3$^{+/-}$	92.5±2.1%	97.0±1.0%	83.7±4.0%	n/a	n/a

Type I	α1(I)707				
	T	B	Sk	Co	Sc
Sc65$^{-/-}$	65.0±8.0%	17.3±4.0%	3.3±2.1%	30.3±11%	33.0±11%
Sc65$^{+/+}$	63.8±11%	14.3±6.8%	5.0±1.0%	26.3±7.6%	38.0±7.5%
P3h3$^{-/-}$	60.8±7.2%	14.3±3.5%	3.3±0.3%	n/a	n/a
P3h3$^{+/-}$	61.5±4.0%	12.3±2.5%	4.7±1.3%	n/a	n/a

Type I	α1(I) $(GPP)_5$1000-1014				
	T	B	Sk	Co	Sc
Sc65$^{-/-}$	79.0±6.4%	0%	0%	61.7±8.5%	67.7±8.7%
Sc65$^{+/+}$	76.0±7.5%	0%	0%	61.0±1.0%	66.0±5.6%
P3h3$^{-/-}$	77.8±5.2%	0%	0%	n/a	n/a
P3h3$^{+/-}$	79.3±4.3%	0%	0%	n/a	n/a

Type I	α2(I)707				
	T	B	Sk	Co	Sc
Sc65$^{-/-}$	88.3±3.2%	31.0±2.0%	8.7±3.2%	46.7±13%	51.3±11%
Sc65$^{+/+}$	89.5±4.4%	31.7±2.9%	11.3±1.2%	46.7±12%	57.0±6.9%
P3h3$^{-/-}$	90.3±1.5%	19.7±2.1%	10.7±3.1%	n/a	n/a
P3h3$^{+/-}$	90.5±1.7%	19.7±4.0%	9.7±0.6%	n/a	n/a

Type II	α1(II)986	α1(II)944	Type V	α2(V)986	α2(V)944
	Cart	Cart		B	B
[a]*Sc65*$^{-/-}$	77.0±2.8%	61.5±9.2%	*Sc65*$^{-/-}$	98.7±0.3%	66.0±2.6%
[a]*Sc65*$^{+/+}$	81.5±9.2%	46.5±9.2%	*Sc65*$^{+/+}$	98.5±0.3%	61.7±1.5%
[b]*P3h3*$^{-/-}$	80%	75%	*P3h3*$^{-/-}$	98.7±0.7%	70.0±10%
[b]*P3h3*$^{+/-}$	80%	75%	*P3h3*$^{+/-}$	98.7±0.7%	74.3±4.9%

Type IV	α1(IV)602	α2(IV)197	α1(IV)1440
	K	K	K
[b]*Sc65*$^{-/-}$	70%	45%	55%
[b]*Sc65*$^{+/+}$	70%	45%	55%
[b]*P3h3*$^{-/-}$	65%	35%	50%
[b]*P3h3*$^{+/-}$	65%	35%	50%

the cause was α1-α1 C-telopeptide aldol formation due to enhanced lysyl oxidase oxidation of α1-C-telopeptide lysines (22). Further studies suggested that fibromodulin interacts with lysyl oxidase supporting this conclusion (23). Interestingly, the shift in band intensity in the current mice was most prominent in skin, less so in tendon, and absent in bone collagen extracts.

Differences in native collagen extractability in 3% acetic acid from lyophilized tissue samples supported an effect on stable intermolecular cross-linking in non-mineralized *P3h3*$^{-/-}$ tissue collagens. Densitometry of the combined stained α-, β-, and γ-chains resolved on SDS-PAGE revealed that *P3h3*$^{-/-}$ skin collagen ($n = 4$) was 41% more extractable than control skin collagen ($n = 2$). Similarly, *P3h3*$^{-/-}$ tendon collagen ($n = 3$) was 39% more extractable than control tendon collagen ($n = 2$).

Lack of Effect on Prolyl 3-Hydroxylation—Tandem mass spectrometry was used as a screen to survey the degree of prolyl 3-hydroxylation at all known sites we could readily access as tryptic peptides from collagen types I, II, IV, and V. No significant evidence of suppression was observed at any site in *Sc65*$^{-/-}$ or *P3h3*$^{-/-}$ tissues (Table 1 details the findings). This was surprising, particularly for *P3h3*$^{-/-}$, which is a close homolog of P3h1 and P3h2, including a potentially active catalytic domain. Both P3h1 and P3h2 have evolved preferred GPP substrate sequences in a range of collagen types (17, 24, 25).

Identification of the Molecular Structure of the γ_{112} Trimer—The molecular nature of the γ_{112} trimer was investigated using in-gel trypsin mass spectrometry. Mass spectrometric analysis revealed a prominent dimeric α1(I) C-telopeptide with its cross-linking residue fitting exactly an α,β-unsaturated allysine aldol (Fig. 3*A*). As previously shown, trypsin does not cleave after lysines that have been converted to lysine aldehydes, resulting in 6-residue longer tryptic telopeptides cleaved after arginine (22). Notably, MS after in-gel trypsin digest of the γ_{112} trimer revealed no monomeric α1(I) C-telopeptide, only the cross-linked dimer. MS-MS confirmed the identity of the dimeric cross-linked tryptic peptide (Fig. 3*B*). The +16 Da mass ladder given by the parent ion is the result of variable 4-hydroxylation of the Yaa position Pro in the C-terminal GPP of the triple-helical domain of each α1-chain of the dimer.

Tandem Mass Spectrometry Targeted at α1(I) and α2(I) Cross-linking Lysines Shows Under-hydroxylation—Lysine hydroxylation at the cross-linking site, residue Lys-87, was investigated using tandem mass spectrometry of type I collagen α1(I) chains extracted from bone, skin, tendon, aorta, and cornea. A similar pattern of reduced hydroxylation was observed from both *Sc65*$^{-/-}$ and *P3h3*$^{-/-}$ mouse tissues, but the effect was consistently greater with *Sc65*$^{-/-}$ mice. As previously reported for the *Sc65*$^{-/-}$ mouse, the post-translational shift was more pronounced in skin at helical domain cross-linking residue Lys-87 (Fig. 4) compared with bone. Type I collagen from all soft tissues (skin, tendon, and aorta) showed almost complete loss of post-translational modification of Lys-87 (Table 2). As in the *Sc65*$^{-/-}$ mouse, all helical cross-linking sites appear to be under-hydroxylated in the *P3h3*$^{-/-}$ mouse. Indeed, the α1(I) Lys-930 residue, which is completely hydroxylated in *P3h3*$^{+/-}$ skin, is unmodified in the *P3h3*$^{-/-}$ mouse skin (Fig. 5). A similar loss of hydroxylation was found at Lys-930 in skin, bone, and tendon from both *P3h3*$^{-/-}$ and *Sc65*$^{-/-}$ mice. WT tendon was unique among soft tissues with 100% hydroxylated and

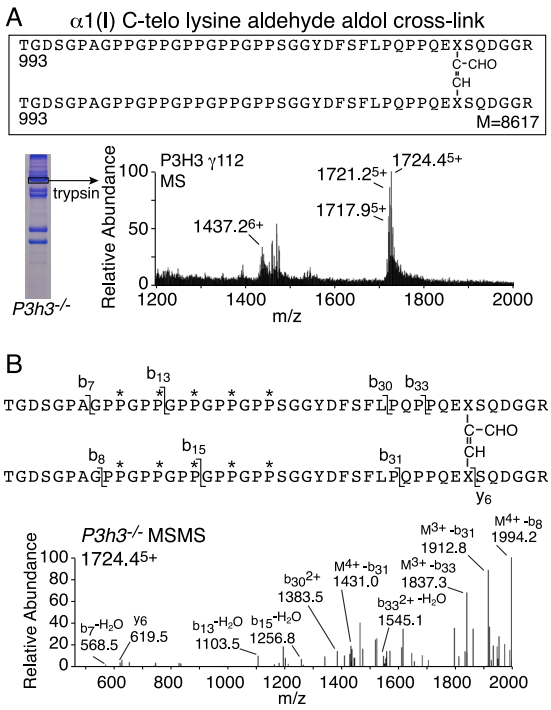

FIGURE 3. **Increased intramolecular C-telopeptide aldol cross-links in knock-out skin type I collagen.** The γ_{112} trimer from *P3h3*$^{-/-}$ mouse skin has a distinct tryptic peptide profile from that of the α1(I) monomer when analyzed using mass spectrometry. *A*, the LC-MS profile of in-gel trypsin digests of the γ_{112} band from *P3h3*$^{-/-}$ mouse skin confirmed the presence of the α1(I) C-telopeptide lysine aldehyde aldol dimer in the γ_{112} band. *B*, MS/MS fragmentation spectrum of the parent ion (1724.4^{5+}) from the *P3h3*$^{-/-}$ γ_{112} band. The trypsin-digested dimeric peptide is shown with P* indicating 4Hyp.

non-glycosylated Lys-87 on both α-chains of type I collagen. The effect on Lys-87 hydroxylation was greater in *Sc65*$^{-/-}$ tendon compared with *P3h3*$^{-/-}$ tendon. The data are compiled in Table 2.

Type V Collagen Under-hydroxylation at Cross-linking Sites Is Restricted to Soft Tissue—The skin dominated reduction in hydroxylation and glycosylation of the helical domain cross-linking lysine 87 was also evident in type V collagen but to a lesser extent than in type I (Table 3). Lys-87 of α1(V) and α2(V) from WT skin was fully hydroxylated and glycosylated as glcgal-Hyl. A mild decrease in these modifications is seen from skin of *Sc65*$^{-/-}$ and *P3h3*$^{-/-}$ mice. As with type I collagen, the effect appeared to be more pronounced in the *Sc65*$^{-/-}$ mouse. In contrast, no post-translational variances were observed in the type V collagen α-chains from bone between WT and *Sc65*$^{-/-}$ or *P3h3*$^{-/-}$ (Table 3).

Altered Aldimine Divalent Cross-linking in Mutant Skin—Bacterial collagenase digests of borohydride-reduced skin were analyzed by mass spectrometry to target the pool of aldimine divalent cross-links in the whole tissue collagen. This approach is useful for tracking structural intermediates in the lysine aldehyde cross-linking pathway. The LC-MS profile of the C-telopeptide to Lys-87 cross-linked peptide from collagenase-digested WT skin shows a fully glycosylated reduced aldimine cross-linked structure between α1(I) Lys-87 and an α1(I) C-telopeptide lysine (Fig. 6*A*). This is consistent with the predominance of glcgal-Hyl at Lys-87 in the linear tryptic peptide from the α1(I) chain extracted from WT skin. From *P3h3*$^{-/-}$ mouse

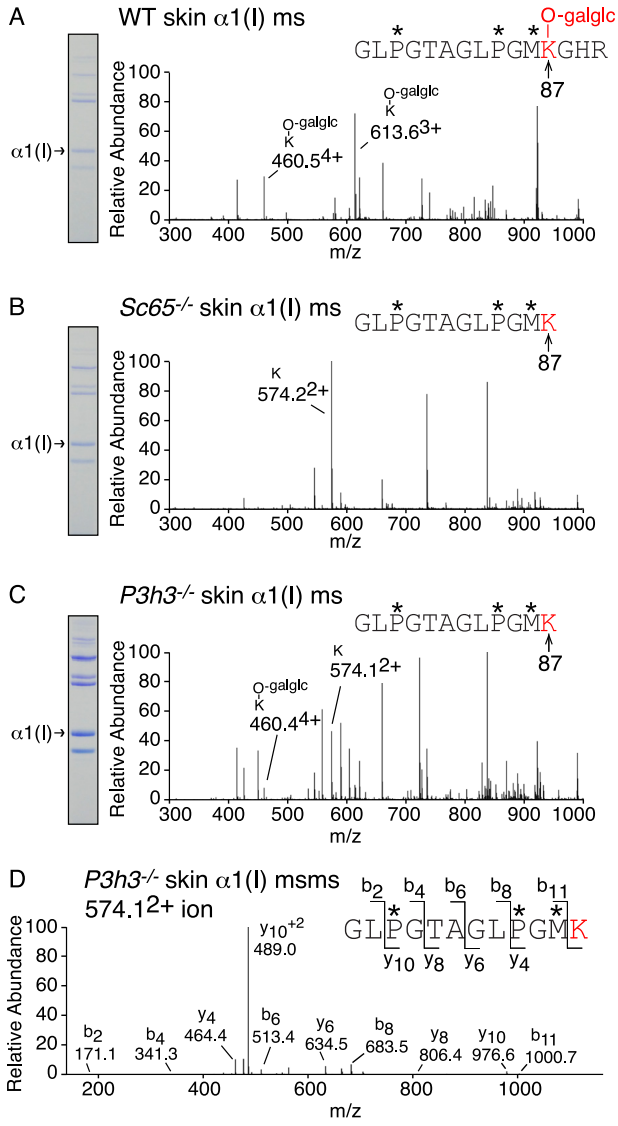

FIGURE 4. **Under-hydroxylation at cross-linking Lys-87 in *P3h3*$^{-/-}$ and *Sc65*$^{-/-}$ skin collagen.** LC-MS profiles of in-gel trypsin digests of the α1(I) collagen chains from WT, *Sc65*$^{-/-}$, and *P3h3*$^{-/-}$ mouse skin. *A*, MS profile of α1(I) from WT mouse skin reveals 100% glucosyl-galactosyl-Hyl (460.5^{4+} and 613.6^{3+}) at residue α1(I) Hyl87. *B*, from *Sc65*$^{-/-}$ mouse skin, Lys-87 is 100% unmodified. Trypsin cleaves after unmodified Lys-87 yielding a smaller tryptic peptide (574.2^{2+}). *C*, from *P3h3*$^{-/-}$ mouse skin, Lys-87 is predominantly unmodified (80% Lys (574.1^{2+}); 20% glucosyl-galactosyl-Hyl (460.4^{4+})). *D*, MS-MS fragmentation spectrum of the parent ion (574.1^{2+}) from *P3h3*$^{-/-}$ skin α1(I). The *b* and *y* ion masses reveal no modifications on α1(I) Lys-87. In-gel trypsin digests typically undergo complete oxidation of methionine residues yielding methionine sulfoxide. The trypsin-generated peptide is shown with *P** indicating 4Hyp, *M** indicating methionine sulfoxide, and *-galglc* indicating glucosyl-galactosyl-.

skin, about equal amounts of the fully glycosylated and a non-glycosylated reduced aldimine cross-link structure were recovered (Fig. 6, *B* and *C*). This finding suggests that glcgal-Hyl at Lys-87 is favored chemically and sterically over Lys and non-glycosylated Hyl as an aldimine end product on the lysine aldehyde cross-linking pathway, as only ~20% of the α1(I) chains from *P3h3*$^{-/-}$ skin were glycosylated at Lys-87 (Fig. 4; Table 2). The total ion current, an index of the amount of the cross-linked peptide in the MS scan, was ~10 times higher for the WT aldimine product compared with the equivalent *P3h3*$^{-/-}$ aldimine products. Although this should be considered only semi-

TABLE 2

Comparison of type I collagen lysine 87 post-translational modifications between tissues

Modifications on lysine 87 from both α-chains of type I collagen in WT, *Sc65*$^{-/-}$, and *P3h3*$^{-/-}$ mice were measured using mass spectrometry in skin, bone, tendon, and aorta. Lysine modifications include unmodified Lys, hydroxylysine (Hyl), galactosyl-hydroxylysine (G-Hyl), and glucosylgalactosyl-hydroxylysine (GG-Hyl). Each percentage was determined based on the ratio of the *m*/*z* peaks of each post-translational variant from a minimum of three mice unless indicated.

		Modification			
	Mouse	Lys	Hyl	G-Hyl	GG-Hyl
Skin					
α1(I) Lys-87	WT				100 ± 0.0%
	Sc65$^{-/-}$	100 ± 0.0%			
	P3h3$^{-/-}$	80.3 ± 3.0%			20.1 ± 1.7%
α2(I) Lys-87	WT	35.7 ± 2.3%	64.3 ± 2.3%		
	Sc65$^{-/-}$	93.7 ± 3.2%	6.3 ± 3.2%		
	P3h3$^{-/-}$	90.0 ± 2.0%	10.0 ± 2.0%		
Bone					
α1(I) Lys-87	WT			21.7 ± 3.8%	78.3 ± 3.8%
	Sc65$^{-/-}$	58.7 ± 12%		15.5 ± 5.5%	25.3 ± 6.4%
	P3h3$^{-/-}$	51.0 ± 5.3%		14.7 ± 2.5%	34.3 ± 3.5%
α2(I) Lys-87	WT	22.5 ± 4.8%	77.5 ± 4.8%		
	Sc65$^{-/-}$	92.7 ± 2.9%	7.3 ± 2.9%		
	P3h3$^{-/-}$	42.7 ± 3.8%	57.3 ± 3.8%		
Tendon					
α1(I) Lys-87	WT		100 ± 0.0%		
	Sc65$^{-/-}$	100 ± 0.0%			
	P3h3$^{-/-}$	47.3 ± 0.3%	52.7 ± 3.8%		
α2(I) Lys-87	WT		100 ± 0.0%		
	Sc65$^{-/-}$	85.5 ± 8.1%	14.5 ± 8.1%		
	P3h3$^{-/-}$	32.3 ± 2.6%	67.8 ± 2.6%		
Aorta					
α1(I) Lys-87	WT				100 ± 0.0%
	Sc65$^{-/-}$	100 ± 0.0%			
	[a]*P3h3*$^{-/-}$	100 ± 0.0%			
α2(I) Lys-87	WT		86.7 ± 4.3%		13.3 ± 4.2%
	Sc65$^{-/-}$	100 ± 0.0%			
	P3h3$^{-/-}$[a]	66.0 ± 4.2%	34.0 ± 4.2%		
Cornea					
α1(I) Lys-87	WT	6.7 ± 11%			93.3 ± 11%
	Sc65$^{-/-}$	51.7 ± 10%	14.0 ± 4.6%		35.0 ± 10%
α2(I) Lys-87	WT	3.7 ± 6.4%	93.0 ± 6.1%		3.3 ± 5.8%
	Sc65$^{-/-}$	57.7 ± 17%	42.3 ± 17%		

[a] Two mice.

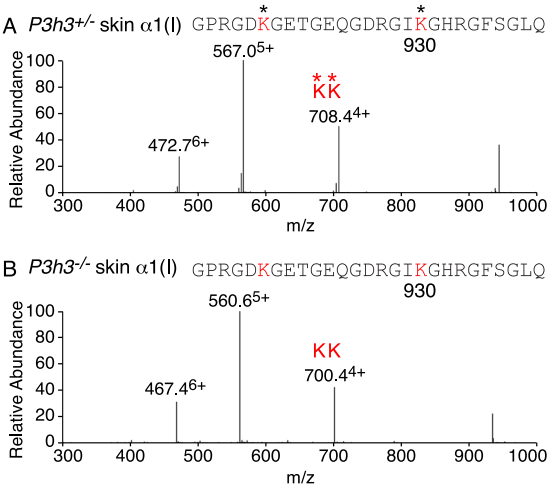

FIGURE 5. **Complete loss of hydroxylation at cross-linking Lys-930 in *P3h3*$^{-/-}$ skin collagen.** LC-MS profiles of peptides containing the helical domain Lys-930 cross-linking site from collagen α1(I) prepared by bacterial collagenase digestion of total dermal collagen. *A,* MS profile from *P3h3*$^{+/-}$ mouse skin reveals 100% lysyl hydroxylation at residue 930 (472.7^{6+}, 567.0^{5+}, and 708.4^{4+}). *B,* in *P3h3*$^{-/-}$ mouse skin, Lys-930 is 100% unmodified (467.4^{6+}, 560.6^{5+}, and 700.4^{4+}). Identical profiles were found at this site in skin, bone, and tendon from both *P3h3*$^{-/-}$ and *Sc65*$^{-/-}$ mice.

quantitative, it suggests that the mutant skin has significantly fewer aldimine cross-links at this site than WT skin. The cross-link between α1(I) Lys-930 and the α1(I)N-telopeptide was fully hydroxylated in WT skin (hydroxylysino-norleucine on reduction) (Fig. 7*A*); however, in *P3h3*$^{-/-}$ mouse skin only the non-hydroxylated aldimine cross-link was identified (lysino-norleucine on reduction) (Fig. 7*B*).

Pyridinoline (HP and LP) Cross-link Analysis—As an independent downstream measure of the effect of the loss of Sc65 or P3H3 on lysine cross-linking, pyridinoline cross-links were quantified after acid hydrolysis of samples of bone, aorta, lung, cartilage, and dentin collagen from each genotype (Table 4). The results showed a significantly lower ratio of HP/LP in bone, aorta, and lung in both knock-out mouse strains. A similar reversal in the HP/LP ratio of the cross-linking pyridinolines of bone and other tissues is seen in patients with Ehlers-Danlos syndrome (EDS) VI (26). A comparable but less marked shift in the HP/LP ratio was found in dentin and cartilage samples from the *Sc65*$^{-/-}$ mice. No genotypic significance can be attached to variations in total content (HP + LP mol/mol of collagen) between samples as shown in Table 4, which may be due to sampling site variability.

Discussion

Although both construct strains of *Sc65*$^{-/-}$ (gene trap and floxed) and *P3h3*$^{-/-}$ mice were indistinguishable by gross physical appearance from their WT littermates, the mutant skins lacked the structural integrity of normal skin on dissection. It is notable that increased skin fragility and low bone mass were quantified in the *Sc65*$^{-/-}$ mouse strain compared with WT littermates (21). On mass spectrometric analysis, type I collagen from both *Sc65*$^{-/-}$ and *P3h3*$^{-/-}$ tissues revealed

TABLE 3

Summary of posttranslational variances in linear cross-linking lysine 87 from type V collagens

Modifications on lysine 87 from both α-chains of type V collagen in WT, *Sc65*$^{-/-}$, and *P3h3*$^{-/-}$ mice were measured using mass spectrometry in skin and bone. Lysine modifications include unmodified Lys, hydroxylysine (Hyl), galactosyl-hydroxylysine (G-Hyl), and glucosylgalactosyl-hydroxylysine (GG-Hyl). Each percentage was determined based on the ratio of the m/z peaks of each post-translational variant from a minimum of three mice unless indicated.

		Modification			
	Mouse	Lys	Hyl	G-Hyl	GG-Hyl
Skin					
α1(V) Lys-87	WT				100 ± 0.0%
	Sc65$^{-/-}$	33.7 ± 14%			66.3 ± 14%
	P3h3$^{-/-a}$	23.0 ± 4.2%			77.0 ± 4.2%
α2(V) Lys-87	WT		25.3 ± 4.9%		74.7 ± 4.9%
	Sc65$^{-/-}$	19.3 ± 10%	26.0 ± 5.2%		54.7 ± 5.7%
	P3h3$^{-/-a}$	17.5 ± 0.7%	24.0 ± 7.1%		59.0 ± 8.5%
Bone					
α1(V) Lys-87	WT				100 ± 0.0%
	Sc65$^{-/-}$				100 ± 0.0%
	P3h3$^{-/-a}$				100 ± 0.0%
α2(V) Lys-87	WT		15 ± 2.6%		85.0 ± 2.6%
	Sc65$^{-/-}$		17.7 ± 10%		82.3 ± 10%
	P3h3$^{-/-a}$		18.5 ± 4.9%		81.5 ± 4.9%

[a] Two mice.

severe under-hydroxylation of lysine residues at triple-helical domain cross-linking sites for skin, tendon, cornea, and aorta. In addition to under-hydroxylation, the residual Hyl87 was under-glycosylated compared with WT for skin, aorta, and cornea. Type V collagen from null mouse skin and aorta exhibited a decrease in hydroxylation/glycosylation at Lys-87 compared with WT; however, no change was detected in type V collagen from null-bone *versus* WT bone. As collagen type V acts as a quantitatively minor but essential template for type I collagen heterofibril polymerization, it is possible that even a minor disturbance in collagen V cross-linking could be amplified in the mature fibril.

The present phenocopied effects on collagen lysine hydroxylation can best be explained if Sc65 and P3H3 form a complex in the ER that is required to facilitate access of LH1 to substrate lysine residues on newly made collagen chains. We proposed an interaction complex that at least transiently involves LH1, CypB, SC65, and P3H3 (21). Similar to the P3H1/CRTAP/CypB enzyme complex, which is required to 3-hydroxylate Pro-986, the primary site of 3Hyp in type I collagen, all four ER components LH1, CypB, SC65, and P3H3 are essential for normal triple-helix lysine hydroxylation. The requirement of CypB for collagen post-translational modification became clear from the effects of PPIB mutations that cause severe osteogenesis imperfecta. They result in loss of prolyl-hydroxylation at Pro-986 (27) and, in CypB knock-out mice, defective lysine hydroxylation in bone (28) and tendon (29) collagens. Furthermore, we know that FKBP65, another peptidyl prolyl isomerase and ER chaperone, can regulate the activity of LH2 the predicted telopeptide lysine hydroxylase (12, 30, 31).

Tissues from both *P3h2*$^{-/-}$ and *Crtap*$^{-/-}$ mice showed no effect on Lys-87 hydroxylation/glycosylation, ruling out any potential redundancy or compensatory function between P3H3, P3H2, and P3H1 subunits in the ER.[3] In contrast to the functionally interdependent complex P3H1/CRTAP required for Pro-986 3-hydroxylation, P3H3/Sc65 appears to be redundant as a prolyl 3-hydroxylase. We had anticipated that P3H3 would act as a prolyl 3-hydroxylase somewhere on collagen, but despite a broad screen of candidate sites in the common collagens no evidence of an affected site was found (Table 1). Given the recent identification of many low occupancy 3-hydroxyproline sites in type IV (32) and type V (33) collagens, and a long list of genetic types of collagen with GPP triplets, it is possible that a proline substrate for P3H3 remains to be identified. Equally possible is lost enzyme activity over the course of evolution but a retained collagen chaperone function in the ER that optimizes LH1-mediated lysine hydroxylation particularly at helical domain cross-linking sites.

The pathogenic significance of the loss of Pro-986 3-hydroxylation in recessive cases of osteogenesis imperfecta caused by *P3H1, CRTAP*, or *CypB* mutations is still not clear, although absence of the complex as a procollagen chaperone rather than absence of 3Hyp is indicated (34, 35). In this context, the over-hydroxylation of telopeptide lysines seen in the bone collagen of OI patients and mouse models caused by mutations in P3H1, CRTAP, and CypB should be noted.

Hydroxylysines are functionally important in collagen for covalent cross-linking. In type I collagen four triple-helical domain lysine sites (α1(I) Lys-87 and Lys-930; α2(I) Lys-87 and Lys-933) can interact with C- and N-telopeptide lysines after the latter have been converted to aldehyde residues by lysyl oxidase. Tissue-specific differences in collagen cross-linking chemistry and maturation are largely determined in the ER by the lysine hydroxylation state of these specific lysines (Fig. 8*A*).

Based on the present findings, what mechanism can explain the altered pattern (Fig. 2) of cross-linked β- and γ-chains seen on SDS-PAGE of skin collagen from *Sc65*$^{-/-}$ and *P3h3*$^{-/-}$ mice? We believe the latter effect is caused by the lack of glcgal-Hyl at Lys-87 in both α-chains of skin type I collagen. In WT skin, aorta and cornea (>90%), type I collagen α1(I) chains all have fully glycosylated glcgal-Hyl at Lys-87 to which α1(I) C-telopeptide allysines in neighboring four-dimensional staggered molecules normally interact to form aldimine cross-links. When α1(I) and α2(I) Lys-87 are not hydroxylated and so cannot be glycosylated the interaction chemistry changes. If in the same molecule both α1-chain C-telopeptide lysines are converted to aldehydes, then they interact to form an intramolecular aldol cross-link in lieu of the typical intermolecular glyco-

[3] D. M. Hudson and D. R. Eyre, unpublished data.

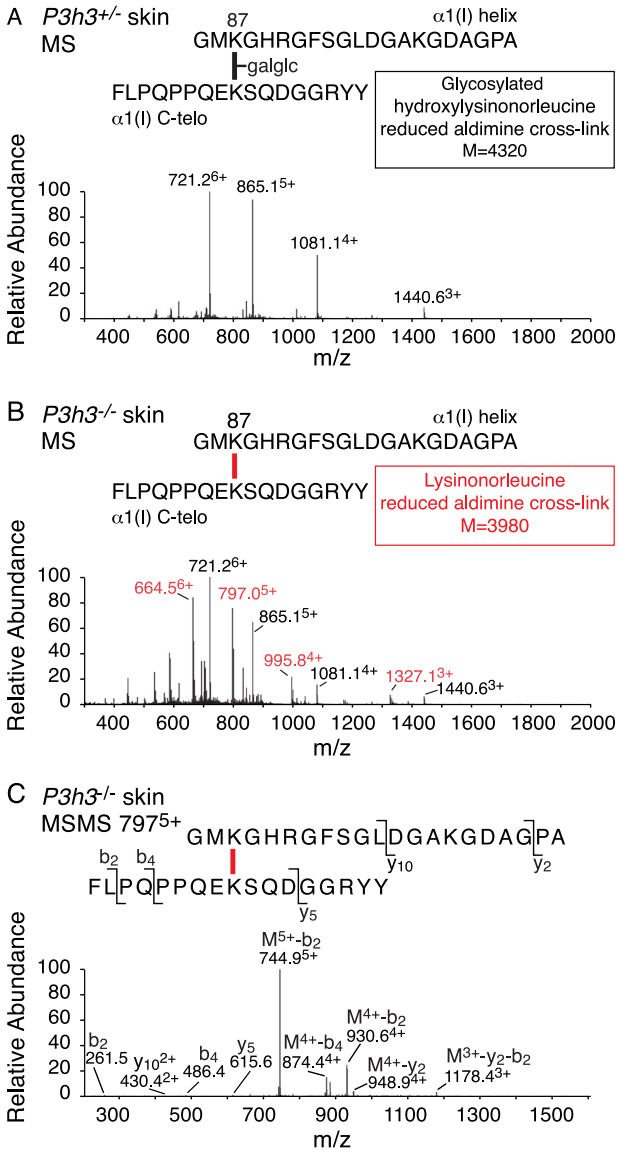

FIGURE 6. **Altered divalent cross-link structure (Lys-87 to C-telopeptide) from *P3h3*$^{-/-}$ mouse skin.** LC-MS profiles of type I collagen divalent cross-linking structures prepared by bacterial collagenase digestion of sodium borohydride-treated skin. *A,* MS profile of a fully glycosylated (glucosyl-galactosyl-) reduced aldimine structure from *P3h3*$^{+/-}$ mouse skin (721.2^{6+}, 865.1^{5+}, 1081.1^{4+}, and 1440.6^{3+}). *B,* from *P3h3*$^{-/-}$ mouse skin, two structures were identified in equal amounts. The same fully glycosylated reduced aldimine found in *P3h3*$^{+/-}$ (721.2^{6+}, 865.1^{5+}, 1081.1^{4+}, and 1440.6^{3+}) plus a non-glycosylated reduced aldimine (664.5^{6+}, 797.0^{5+}, 995.8^{4+}, and 1327.1^{3+}). *C,* MS/MS fragmentation spectrum of the parent ion (797^{5+}) from *P3h3*$^{-/-}$ confirm the mass of the lysine variant from mutant skin. Molecular ions from the lysine and glycosylated hydroxylysine variants are distinguished in *red* and *black*, respectively.

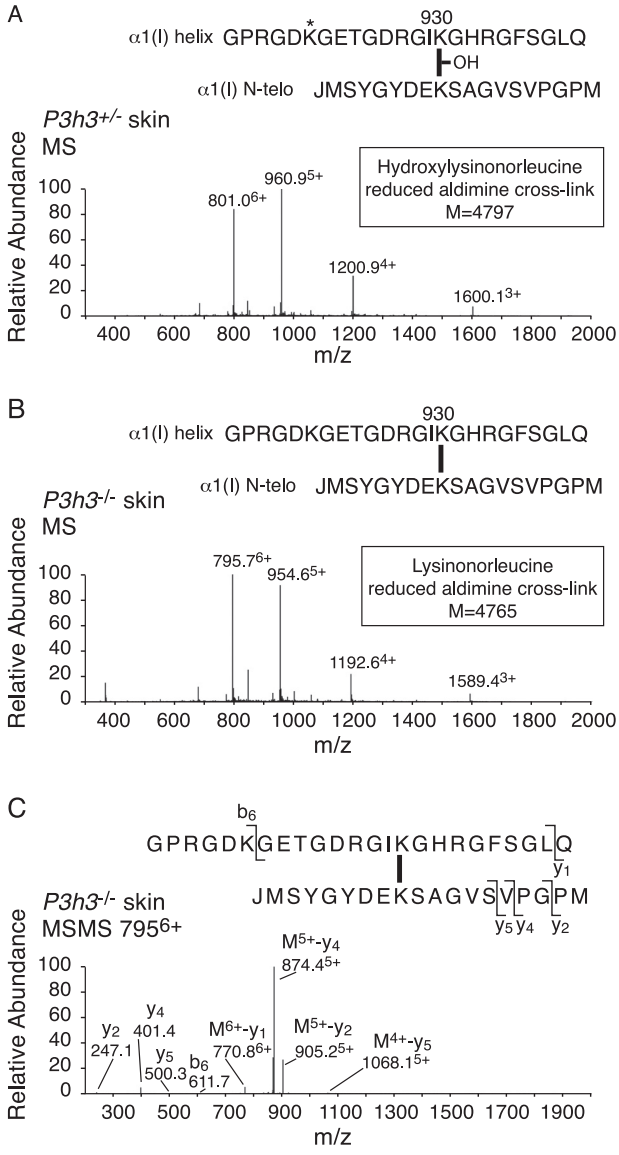

FIGURE 7. **Altered divalent cross-link structure (Lys-930 to N-telopeptide) from *P3h3*$^{-/-}$ mouse skin.** LC-MS profiles of type I collagen divalent cross-linking structures prepared by bacterial collagenase digestion of sodium borohydride-treated skin. *A,* MS profile of a hydroxylated reduced aldimine structure (hydroxylysinonorleucine) from *P3h3*$^{+/-}$ mouse skin (801.0^{6+}, 960.9^{5+}, 1200.9^{4+}, and 1600.1^{3+}). *B,* from *P3h3*$^{-/-}$ mouse skin, only the non-hydroxylated lysine variant (lysinonorleucine) was recovered (795.7^{6+}, 954.6^{5+}, 1192.6^{4+}, and 1589.4^{3+}). *C,* MS/MS fragmentation spectrum of the parent ion (795^{5+}) from *P3h3*$^{-/-}$ mouse skin.

sylated aldimine cross-link present in WT tissue (Fig. 8). Such an abnormal cross-link arrangement for skin can explain the marked increase in γ_{112} trimer and decrease in β_{12} dimer seen on SDS-PAGE (Figs. 2 and 3). It can also explain the increased extractability of type I collagen in non-denaturing 3% acetic acid at 4 °C (~40% more extractable in *P3h3*$^{-/-}$ skin and tendon), if in essence intermolecular C-telopeptide aldols are replaced by intramolecular aldols. Although beyond the scope of the present study it should be noted that major complex cross-links on the allysine aldehyde pathway were reported to be the product of an allysine aldol linked to a histidine by Michael addition and a hydroxylysine by aldimine addition (dehydrohistidinohydroxymerodesmosine (HHMD) on reduction) (36). The structure was based on analyses of acid-hydrolyzed collagen after sodium borohydride reduction, so the native state of the mature aldol cross-linking structures in tissue remains uncertain (37).

The reason why skin appears to be more affected than tendon collagen is probably related to the lack of glcgal-Hyl at Lys-87 in normal mature tendon type I collagen. To speculate, the combined loss of hydroxylation and glycosylation at Lys-87 of skin, aorta, and cornea may have the above summarized effect on C-telopeptide aldol placement but not in

TABLE 4

Altered mature cross-linking in *P3h3*$^{-/-}$ and *Sc65*$^{-/-}$ mouse tissues

Concentration of pyridinoline cross-linking residues in mouse bone, aorta, lung, dentin, and cartilage expressed as moles/mole of collagen (HP, hydroxylysylpyridinoline; LP, lysylpyridinoline). Values were calculated from a minimum of three mice unless indicated.

	HP + LP	HP/LP molar ratio
Bone		
WT[a]	0.29 ± 0.19	7.75 ± 3.46
Sc65$^{-/-}$	0.34 ± 0.02	0.27 ± 0.06
P3h3$^{-/-a}$	0.57 ± 0.03	0.40 ± 0.00
Aorta		
WT[a]	0.59 ± 0.01	12.5 ± 1.41
Sc65$^{-/-b}$	0.78	0.40
P3h3$^{-/-a}$	0.79 ± 0.19	0.60 ± 0.00
Lung		
WT[b]	0.86	14.5
Sc65$^{-/-a}$	0.97 ± 0.40	1.55 ± 1.06
P3h3$^{-/-a}$	1.92 ± 0.86	4.10 ± 2.97
Dentin		
WT[b]	0.85	2.6
Sc65$^{-/-b}$	0.94	1.4
Cartilage		
WT[b]	2.0	4.5
Sc65$^{-/-b}$	2.1	2.8

[a] Two mice.
[b] One mouse.

tendon, which normally has Hyl alone at Lys-87 with no attached sugars. It is notable that the band pattern of WT tendon collagen on SDS-PAGE (Fig. 2) resembles that of *Sc65*$^{-/-}$ and *P3h3*$^{-/-}$ skin with a prominent γ_{112} trimer and with no obvious difference from *Sc65*$^{-/-}$ and *P3h3*$^{-/-}$ tendons. In a sense, therefore, the effect in null mice on skin collagen is to make it resemble normal tendon collagen at this cross-link site. However, with that in mind, normal tendon collagen in a study of fibromodulin-null mice was shown to have incomplete C-telopeptide lysine conversion to aldehydes, a restriction that was lifted in the fibromodulin-null mice (22). It was speculated that in fibromodulin-null mice an increase in collagen molecules with two C-telopeptide allysines produced an observed increase in C-telopeptide aldols and γ_{112} trimers (22).

The observed effects on collagen lysine hydroxylation and cross-linking closely resemble those observed in tissues of EDS VIA patients. Of the many defined clinical subtypes of EDS, most are characterized by skin hyper-extensibility, joint hypermobility, and connective tissue fragility. The kyphoscoliotic type, EDS VIA, is caused by homozygous or compound heterozygous mutations in the PLOD1 gene (encodes LH1). Clinical features of patients with this EDS subtype include progressive kyphoscoliosis, soft velvety skin, muscle hypotonia, arterial ruptures, and fragility of ocular tissues often leading to rupture of the globe and retinal detachment (38, 39). Similar to *Sc65*$^{-/-}$ and *P3h3*$^{-/-}$ mice, the LH1 knock-out (*Plod1*$^{-/-}$) mouse seemed to have milder consequences than Plod1 human cases. For example, muscle hypotonia and aortic ruptures were reported in the *Plod1*$^{-/-}$ mouse but not kyphoscoliosis or skin laxity (40). Despite *Sc65*$^{-/-}$ and *P3h3*$^{-/-}$ mice having at this stage primarily a biochemical phenotype, the potential is clear for suppressed lysine hydroxylation to manifest as an EDS variant in humans.

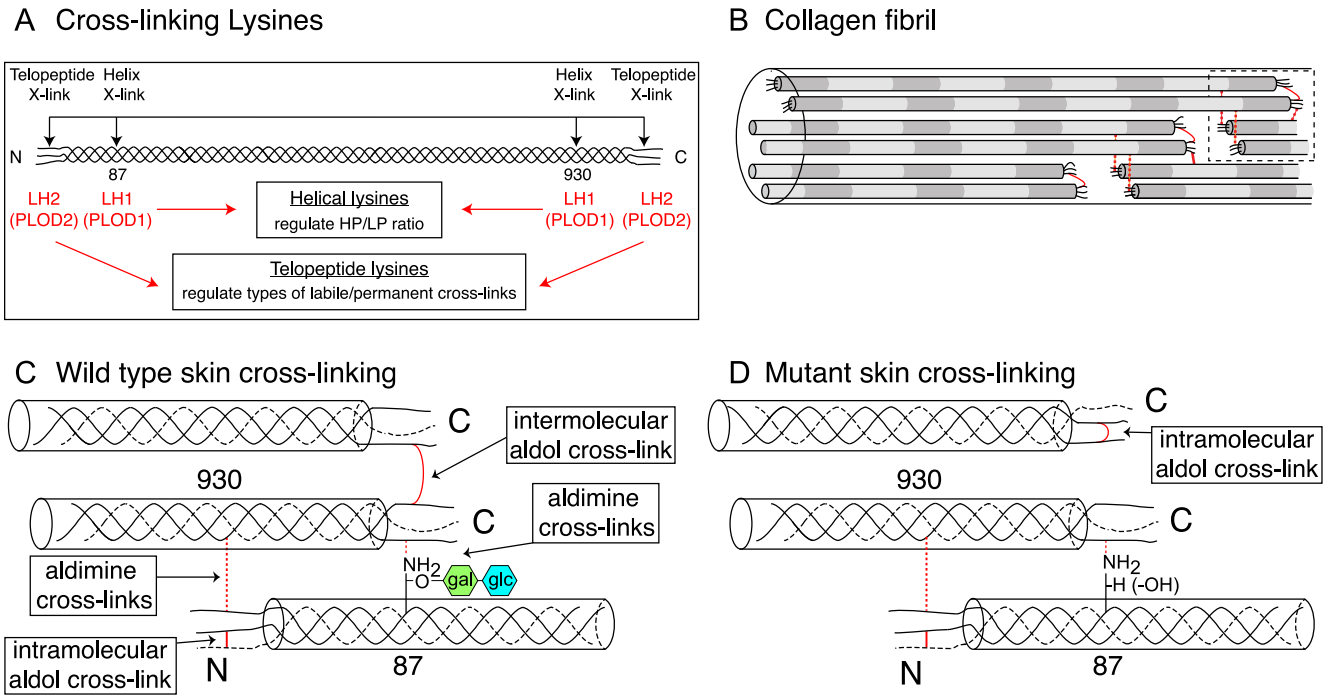

FIGURE 8. **Model speculating how collagen cross-link formation is affected in *P3h3*$^{-/-}$ and *Sc65*$^{-/-}$ mouse skin.** Under normal conditions, LH1 catalyzes the hydroxylation of helical lysines 87 and 930; and LH2 catalyzes the hydroxylation of the N- and C-telopeptide lysines (*A*). In the fibril, collagen molecules are spatially arranged such that intermolecular cross-link placement is optimal (*B*). In WT skin, fully glycosylated Hyl87 preferentially forms an intermolecular aldimine cross-link with a C-telopeptide lysine aldehyde (*C*). In the *P3h3*$^{-/-}$ and *Sc65*$^{-/-}$ mouse tissues the LH1 substrates are under-hydroxylated and subsequently under-glycosylated, which alters collagen cross-linking chemistry (*D*). From mutant skin the results are consistent with the C-telopeptide lysine aldehydes preferentially forming intramolecular aldol cross-links (as opposed to intermolecular aldols). We predict that under normal conditions the presence of the disaccharide on Hyl87 favors aldimine formation with a single C-telopeptide aldehyde and hinders intramolecular aldol formation with a second α1(I) C-telopeptide from the same molecule as the first one, so favoring intermolecular interactions. The net effect of under-hydroxylated Lys-87 then would be fewer stable aldol intermolecular cross-links within and between fibrils.

Experimental Procedures

Production of Knock-out Mice—The *P3h3* knock-out ($P3h3^{-/-}$) mouse was generated using embryonic stem cells obtained from the Knock-out Mouse Project (KOMP) repository. Embryonic stem cells were injected in-house to generate the heterozygous knock-out mice ($P3h3^{+/-}$). Mice were maintained on a C57/BL6J background and were housed in the Baylor College of Medicine vivarium. Genotyping was performed using primers for the WT allele, 5′-TGGAGAACGTGTCAAATTGGAATG-3′ and 5′-TCCATCTGCTCTTCGTATCTGAAAG-3′. The mutant allele was identified by primers, 5′-CGTGGGTAGATGAACGTGTG-3′ and 5′-CTGTCCTAGCTTCCTCACTG-3′.

Tissues from two strains of $Sc65^{-/-}$ mice (19, 21) were analyzed in comparison to $P3h3^{-/-}$ and respective WT tissues. Briefly, for the initial strain the embryonic stem cell clone (129X1/SvJ × 129S1) with a proviral insertion (gene-trap) in the *Sc65* gene was purchased from the Gene Trap Resource of the Phenogenomics Toronto Center (Toronto, Canada). C57/BL6J blastocysts were injected with ES cells and chimeric mice were generated (19). The second $Sc65^{-/-}$ strain employed a conditional targeting construct (using the vector p-flrt-neo-2XloxP) that was designed to introduce loxP sites flanking the last 2 exons (7 and 8) of *Sc65* (floxed mouse). Chimeric mice were generated by electroporating the construct into mouse ES cells derived from F1(C57B6/jx129sv) embryos. Global *Sc65* excision was achieved by mating male Sc65 mice carrying a floxed allele with Hprt-Cre females (21). The use of the latter laboratory mice was approved by the University of Arkansas for Medical Sciences IACUC committee. All mice used in this study had the same genetic background. The reported post-translational variances did not appear to be related to the age or sex of the animals tested.

Collagen Extraction—Type I collagen was solubilized from bone, skin, tendon, aorta, sclera, and cornea by heat denaturation for 5 min at 100 °C in Laemmli buffer (SDS extraction), 3% acetic acid at 4 °C for 24 h, or cyanogen bromide digestion in 70% formic acid at room temperature for 24 h. Type II collagen (rib cage cartilage), type IV collagen (kidney cortex), and type V collagen (bone and skin) α-chains were solubilized by pepsin digestion or cyanogen bromide digestion as previously described (17, 41). Collagen α-chains were resolved by SDS-PAGE and stained with Coomassie Blue R-250. Collagen extractability was determined using NIH ImageJ software as previously described (22).

P3h3 Immunoblot—Human fetal control cartilage tissue was obtained from a National Institutes of Health-sponsored institutional resource (Birth Defects Research Laboratory, University of Washington) (42). $P3h3^{-/-}$ and control whole mouse kidneys were homogenized in saline with protease inhibitors (50 mM Tris-HCl, pH 7.5, 0.15 M NaCl, 2 mM PMSF, 10 mM phenanthroline). An intracellular fraction was solubilized from this tissue extract in SDS sample buffer at 95 °C. Human fetal control cartilage was 4 M guanidine-HCl extracted as previously described (42). Equal loads of total protein were resolved on a 7.5% SDS-PAGE and transblotted to PVDF membrane. Membranes were blocked in 5% milk, probed with P3h3 polyclonal antibody (1:500 dilution, ProteinTech, catalog number 16023-1-AP), and detected with an HRP-conjugated secondary antibody (1:5000, anti-rabbit). Blots were developed using Super-Signal West Pico Chemiluminescent Substrate (Thermo Scientific) and exposed on autoradiography film.

H&E Staining—Skins and femurs were harvested from a 2-month-old mouse and fixed in 10% buffered formalin. Femurs were decalcified with 14% EDTA for 2 weeks before paraffin embedding processing. Paraffin-embedded skin and femur were sectioned (6 micrometer) and the sections were used for H&E staining.

Mass Spectral Analysis of Site-specific Post-translational Modifications—The post-translational modifications 3-hydroxyproline, 5-hydroxylysine (Hyl), glcgal-Hyl, and gal-Hyl glycosides were quantified at specific sites in collagen α-chains as previously described (41). Collagen α-chains were cut from SDS-PAGE gels and subjected to in-gel trypsin digestion. Skin was also digested with bacterial collagenase with and without borohydride reduction as previously described (21) and total collagenase digests were resolved into peptide fractions by C8 reverse-phase HPLC and individual fractions were analyzed by mass spectrometry (43). Electrospray mass spectrometry was carried out on the trypsin- and collagenase-digested peptides using an LTQ XL linear quadrapole ion-trap mass spectrometer equipped with in-line Accela 1250 liquid chromatography and automated sample injection (ThermoFisher Scientific). Proteome Discoverer software (ThermoFisher Scientific) was used for peptide identification. Tryptic peptides were also identified manually by calculating the possible MS-MS ions and matching these to the actual MS-MS spectrum using Thermo Xcalibur software. Hydroxyl differences were determined manually by averaging the full scan MS over several LC-MS minutes to include all the post-translational variations of a given peptide. Protein sequences used for MS analysis were obtained from the Ensembl genome database.

Collagen Cross-linking Analysis—The pyridinoline cross-link content of collagen in bone, dentin, cartilage, and aorta samples was determined by HPLC after acid hydrolysis in 6 M HCl for 24 h at 108 °C. Dried samples were dissolved in 1% (v/v) *n*-heptafluorobutyric acid for quantitation of lysyl pyridinoline (LP) and hydroxylysyl pyridinoline (HP) by reverse-phase HPLC and fluorescence monitoring as previously described (7).

Author Contributions—D. R. E., B. L., and R. M. conceived the idea for the project. J. R., D. M. H., and M. A. W. conducted most of the experiments. K. S. J. generated the $P3h3^{-/-}$ mouse. R. M. and M. D. generated the $Sc65^{-/-}$ mouse. D. M. H., M. A. W., and D. R. E. analyzed the results. D. M. H. and D. R. E. wrote the initial draft of the paper and all authors contributed to the revisions and reviewed the final submitted version.

References

1. Myllyharju, J., and Kivirikko, K. I. (2004) Collagens, modifying enzymes and their mutations in humans, flies and worms. *Trends Genet.* **20,** 33–43
2. Bella, J. (2016) Collagen structure: new tricks from a very old dog. *Biochem. J.* **473,** 1001–1025
3. Hudson, D. M., and Eyre, D. R. (2013) Collagen prolyl 3-hydroxylation: a major role for a minor post-translational modification? *Connect. Tissue Res.* **54,** 245–251

4. Yamauchi, M., and Sricholpech, M. (2012) Lysine post-translational modifications of collagen. *Essays Biochem.* **52,** 113–133
5. Eyre, D. R., and Weis, M. A. (2013) Bone collagen: new clues to its mineralization mechanism from recessive osteogenesis imperfecta. *Calcif. Tissue Int.* **93,** 338–347
6. Eyre, D. R., Paz, M. A., and Gallop, P. M. (1984) Cross-linking in collagen and elastin. *Annu. Rev. Biochem.* **53,** 717–748
7. Eyre, D. (1987) Collagen cross-linking amino acids. *Methods Enzymol.* **144,** 115–139
8. Marini, J. C., Reich, A., and Smith, S. M. (2014) Osteogenesis imperfecta due to mutations in non-collagenous genes: lessons in the biology of bone formation. *Curr. Opin. Pediatr.* **26,** 500–507
9. Ishikawa, Y., Wirz, J., Vranka, J. A., Nagata, K., and Bächinger, H. P. (2009) Biochemical characterization of the prolyl 3-hydroxylase 1·cartilage-associated protein·cyclophilin B complex. *J. Biol. Chem.* **284,** 17641–17647
10. Ha-Vinh, R., Alanay, Y., Bank, R. A., Campos-Xavier, A. B., Zankl, A., Superti-Furga, A., and Bonafé, L. (2004) Phenotypic and molecular characterization of Bruck syndrome (osteogenesis imperfecta with contractures of the large joints) caused by a recessive mutation in PLOD2. *Am. J. Med. Genet. Part A.* **131,** 115–120
11. Barnes, A. M., Cabral, W. A., Weis, M., Makareeva, E., Mertz, E. L., Leikin, S., Eyre, D., Trujillo, C., and Marini, J. C. (2012) Absence of FKBP10 in recessive type XI osteogenesis imperfecta leads to diminished collagen cross-linking and reduced collagen deposition in extracellular matrix. *Hum. Mutat.* **33,** 1589–1598
12. Schwarze, U., Cundy, T., Pyott, S. M., Christiansen, H. E., Hegde, M. R., Bank, R. A., Pals, G., Ankala, A., Conneely, K., Seaver, L., Yandow, S. M., Raney, E., Babovic-Vuksanovic, D., Stoler, J., Ben-Neriah, Z., *et al.* (2013) Mutations in FKBP10, which result in Bruck syndrome and recessive forms of osteogenesis imperfecta, inhibit the hydroxylation of telopeptide lysines in bone collagen. *Hum. Mol. Genet.* **22,** 1–17
13. Mordechai, S., Gradstein, L., Pasanen, A., Ofir, R., El Amour, K., Levy, J., Belfair, N., Lifshitz, T., Joshua, S., Narkis, G., Elbedour, K., Myllyharju, J., and Birk, O. S. (2011) High myopia caused by a mutation in LEPREL1, encoding prolyl 3-hydroxylase 2. *Am. J. Hum. Genet.* **89,** 438–445
14. Guo, H., Tong, P., Peng, Y., Wang, T., Liu, Y., Chen, J., Li, Y., Tian, Q., Hu, Y., Zheng, Y., Xiao, L., Xiong, W., Pan, Q., Hu, Z., and Xia, K. (2014) Homozygous loss-of-function mutation of the LEPREL1 gene causes severe non-syndromic high myopia with early-onset cataract. *Clin. Genet.* **86,** 575–579
15. Khan, A. O., Aldahmesh, M. A., Alsharif, H., and Alkuraya, F. S. (2015) Recessive mutations in LEPREL1 underlie a recognizable lens subluxation phenotype. *Ophthalmic Genet.* **36,** 58–63
16. Pokidysheva, E., Boudko, S., Vranka, J., Zientek, K., Maddox, K., Moser, M., Fässler, R., Ware, J., and Bächinger, H. P. (2014) Biological role of prolyl 3-hydroxylation in type IV collagen. *Proc. Natl. Acad. Sci. U.S.A.* **111,** 161–166
17. Hudson, D. M., Joeng, K. S., Werther, R., Rajagopal, A., Weis, M., Lee, B. H., and Eyre, D. R. (2015) Post-translationally abnormal collagens of prolyl 3-hydroxylase-2 null mice offer a pathobiological mechanism for the high myopia linked to human LEPREL1 mutations. *J. Biol. Chem.* **290,** 8613–8622
18. Tiainen, P., Pasanen, A., Sormunen, R., and Myllyharju, J. (2008) Characterization of recombinant human prolyl 3-hydroxylase isoenzyme 2, an enzyme modifying the basement membrane collagen IV. *J. Biol. Chem.* **283,** 19432–19439
19. Gruenwald, K., Castagnola, P., Besio, R., Dimori, M., Chen, Y., Akel, N. S., Swain, F. L., Skinner, R. A., Eyre, D. R., Gaddy, D., Suva, L. J., and Morello, R. (2014) Sc65 is a novel endoplasmic reticulum protein that regulates bone mass homeostasis. *J. Bone Miner. Res.* **29,** 666–675
20. Cavazzini, F., Magistroni, R., Furci, L., Lupo, V., Ligabue, G., Granito, M., Leonelli, M., Albertazzi, A., and Cappelli, G. (2012) Identification and characterization of a new autoimmune protein in membranous nephropathy by immunoscreening of a renal cDNA library. *PloS One* **7,** e48845
21. Heard, M. E., Besio, R., Weis, M., Rai, J., Hudson, D. M., Dimori, M., Zimmerman, S. M., Kamykowski, J. A., Hogue, W. R., Swain, F. L., Burdine, M. S., Mackintosh, S. G., Tackett, A. J., Suva, L. J., Eyre, D. R., and Morello, R. (2016) Sc65-null mice provide evidence for a novel endoplasmic reticulum complex regulating collagen lysyl hydroxylation. *PLoS Genet.* **12,** e1006002
22. Kalamajski, S., Liu, C., Tillgren, V., Rubin, K., Oldberg, Å., Rai, J., Weis, M., and Eyre, D. R. (2014) Increased C-telopeptide cross-linking of tendon type I collagen in fibromodulin-deficient mice. *J. Biol. Chem.* **289,** 18873–18879
23. Kalamajski, S., Bihan, D., Bonna, A., Rubin, K., and Farndale, R. W. (2016) Fibromodulin interacts with collagen cross-linking sites and activates lysyl oxidase. *J. Biol. Chem.* **291,** 7951–7960
24. Hudson, D. M., Werther, R., Weis, M., Wu, J.-J., and Eyre, D. R. (2014) Evolutionary origins of C-terminal (GPP)n 3-hydroxyproline formation in vertebrate tendon collagen. *PLoS One* **9,** e93467
25. Pokidysheva, E., Zientek, K. D., Ishikawa, Y., Mizuno, K., Vranka, J. A., Montgomery, N. T., Keene, D. R., Kawaguchi, T., Okuyama, K., and Bächinger, H. P. (2013) Posttranslational modifications in type I collagen from different tissues extracted from wild type and prolyl 3-hydroxylase 1 null mice. *J. Biol. Chem.* **288,** 24742–24752
26. Steinmann, B., Eyre, D. R., and Shao, P. (1995) Urinary pyridinoline cross-links in Ehlers-Danlos syndrome type VI. *Am. J. Hum. Genet.* **57,** 1505–1508
27. Barnes, A. M., Carter, E. M., Cabral, W. A., Weis, M., Chang, W., Makareeva, E., Leikin, S., Rotimi, C. N., Eyre, D. R., Raggio, C. L., and Marini, J. C. (2010) Lack of cyclophilin B in osteogenesis imperfecta with normal collagen folding. *N. Engl. J. Med.* **362,** 521–528
28. Cabral, W. A., Perdivara, I., Weis, M., Terajima, M., Blissett, A. R., Chang, W., Perosky, J. E., Makareeva, E. N., Mertz, E. L., Leikin, S., Tomer, K. B., Kozloff, K. M., Eyre, D. R., Yamauchi, M., and Marini, J. C. (2014) Abnormal type I collagen post-translational modification and crosslinking in a cyclophilin B KO mouse model of recessive osteogenesis imperfecta. *PLoS Genet.* **10,** e1004465
29. Terajima, M., Taga, Y., Chen, Y., Cabral, W. A., Hou-Fu, G., Srisawasdi, S., Nagasawa, M., Sumida, N., Hattori, S., Kurie, J. M., Marini, J. C., and Yamauchi, M. (2016) Cyclophilin-B modulates collagen cross-linking by differentially affecting lysine hydroxylation in the helical and telopeptidyl domains of tendon type I collagen. *J. Biol. Chem.* **291,** 9501–9512
30. Lietman, C. D., Rajagopal, A., Homan, E. P., Munivez, E., Jiang, M.-M., Bertin, T. K., Chen, Y., Hicks, J., Weis, M., Eyre, D., Lee, B., and Krakow, D. (2014) Connective tissue alterations in Fkbp10$^{-/-}$ mice. *Hum. Mol. Genet.* **23,** 4822–4831
31. Gjaltema, R. A., van der Stoel, M. M., Boersema, M., and Bank, R. A. (2016) Disentangling mechanisms involved in collagen pyridinoline cross-linking: the immunophilin FKBP65 is critical for dimerization of lysyl hydroxylase 2. *Proc. Natl. Acad. Sci. U.S.A.* **113,** 7142–7147
32. Basak, T., Vega-Montoto, L., Zimmerman, L. J., Tabb, D. L., Hudson, B. G., and Vanacore, R. M. (2016) Comprehensive characterization of glycosylation and hydroxylation of basement membrane collagen IV by high-resolution mass spectrometry. *J. Proteome Res.* **15,** 245–258
33. Yang, C., Park, A. C., Davis, N. A., Russell, J. D., Kim, B., Brand, D. D., Lawrence, M. J., Ge, Y., Westphall, M. S., Coon, J. J., and Greenspan, D. S. (2012) Comprehensive mass spectrometric mapping of the hydroxylated amino acid residues of the α1(V) collagen chain. *J. Biol. Chem.* **287,** 40598–40610
34. Hudson, D. M., Kim, L. S., Weis, M., Cohn, D. H., and Eyre, D. R. (2012) Peptidyl 3-hydroxyproline binding properties of type I collagen suggest a function in fibril supramolecular assembly. *Biochemistry* **51,** 2417–2424
35. Homan, E. P., Lietman, C., Grafe, I., Lennington, J., Morello, R., Napierala, D., Jiang, M.-M., Munivez, E. M., Dawson, B., Bertin, T. K., Chen, Y., Lua, R., Lichtarge, O., Hicks, J., Weis, M. A., Eyre, D., and Lee, B. H. (2014) Differential effects of collagen prolyl 3-hydroxylation on skeletal tissues. *PLoS Genet.* **10,** e1004121
36. Tanzer, M. L., Housley, T., Berube, L., Fairweather, R., Franzblau, C., and Gallop, P. M. (1973) Structure of two histidine-containing crosslinks from collagen. *J. Biol. Chem.* **248,** 393–402
37. Robins, S. P., and Bailey, A. J. (1973) The chemistry of the collagen cross-links: the characterization of fraction C, a possible artifact produced during the reduction of collagen fibres with borohydride. *Biochem. J.* **135,** 657–665

38. Steinmann, B., Royce, P. M., and Superti-Furga, A. (2002) The Ehlers-Danlos Syndrome. in *Connective Tissue and Its Heritable Disorders*, pp. 431–523, John Wiley & Sons, Inc., Hoboken, NJ
39. Steinmann, B., Royce, P. M., and Superti-Furga, A. (2003) in *Connective Tissue and Its Heritable Disorders* (Royce, P. M., and Steinman, B., eds), pp. 431–523, John Wiley & Sons, Inc., New York
40. Takaluoma, K., Hyry, M., Lantto, J., Sormunen, R., Bank, R. A., Kivirikko, K. I., Myllyharju, J., and Soininen, R. (2007) Tissue-specific changes in the hydroxylysine content and cross-links of collagens and alterations in fibril morphology in lysyl hydroxylase 1 knock-out mice. *J. Biol. Chem.* **282,** 6588–6596
41. Weis, M. A., Hudson, D. M., Kim, L., Scott, M., Wu, J. J., and Eyre, D. R. (2010) Location of 3-hydroxyproline residues in collagen types I, II, III, and V/XI implies a role in fibril supramolecular assembly. *J. Biol. Chem.* **285,** 2580–2590
42. Matsui, Y., Wu, J.-J., Weis, M. A., Pietka, T., and Eyre, D. R. (2003) Matrix deposition of tryptophan-containing allelic variants of type IX collagen in developing human cartilage. *Matrix Biol.* **22,** 123–129
43. Hanson, D. A., and Eyre, D. R. (1996) Molecular site specificity of pyridinoline and pyrrole cross-links in type I collagen of human bone. *J. Biol. Chem.* **271,** 26508–26516